Supporting Information

Combining tetraphenylethene (TPE) derivatives cations with Eu^{3+}-*β*-diketone complex anions for tunable luminescence

Jicao Han, Zhengyu Zhang, Dongdong Liu and Xi Wang*

Marine College, Shandong University, Weihai, Weihai 264209, People's Republic of China.
E-mail: xi_wang@sdu.edu.cn

General information

The raw materials used in the experiment include 1-(bromomethyl) -4- (1,2,2- triphenylethenyl) benzene (Energy Chemical), pyridine (Energy Chemical), europium (III) chloride hexahydrate (Energy Chemical), 4,4,4-trifluoro-1- phenyl-1,3-butanedione (ABM) (Energy Chemical), gadolinium trichloride hexahydrate (Energy Chemical), and citric acid monohydrate (CA) (Aladdin). These starting materials were used without further purification. X-ray photoelectron spectroscopy (XPS) was measured by ThermoEscalab250 spectrometer excited by monochromatic Al-Kα. Powder X-ray diffraction (XRD) data were collected on a Rigaku Ultima IV X-ray diffractometer with Cu Kα radiation (λ=0.15418 nm). The morphology of the related products was observed by TecnaiG2-20 Transmission Electron Microscope (TEM) and Regulus 8100 Scanning Electron Microscope (SEM). ^{1}H NMR spectra were obtained on AVANCE III HD 400 MHz nuclear magnetic resonance spectrometer. UV-Vis spectra were detected on a Hitachi U-2910 spectrophotometer. Fluorescence spectra were recorded on a Hitachi F-7000 spectrometer. Phosphorescence spectra were detected on a FS5 spectrometer. Elemental analysis (C, H, O and N) was performed with a Elemontar Unicube, and the content of Eu^{3+} was obtained by using an inductively coupled plasma mass spectrometer Agilent 7700 Series. Mass spectrum was measured on a mass spectrometer Agilent Q-TOF 6550. Fluorescence lifetime and fluorescence quantum yield were obtained using the steady/transient state fluorescence spectrometer Edinburgh FLS980.

Synthetic Procedures

Synthesis of TPE^+-Br^-

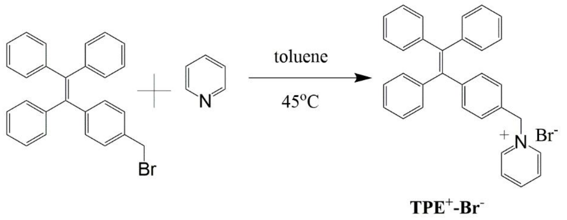

Scheme S1 Synthesis of TPE^+-Br^-

1-(Bromomethyl)-4-(1,2,2-triphenylethenyl) benzene (215 mg, 0.5 mmol) was dissolved in 1.5 mL of toluene in round bottom flask, then the pyridine (0.1 mL, 1.2 mmol) was added into the above reactant, the mixture was then heated and stirred at 45°C for 12 hours. The precipitation was filtered, washed with ethyl ether (3 × 4 mL). Finally, the white solid was obtained. The yield was 85% after vacuum drying. ^{1}H NMR (400 MHz, Chloroform-d) δ 9.46 – 9.40 (m, 2H), 8.38 (td, J = 7.8, 1.3 Hz, 1H), 8.03 – 7.95 (m, 2H), 7.36 – 7.29 (m, 2H), 7.15 – 6.94 (m, 17H), 6.19 (s, 2H).

Synthesis of $(C_2H_5)_3HN^+$-GdL_4^-(L=ABM)

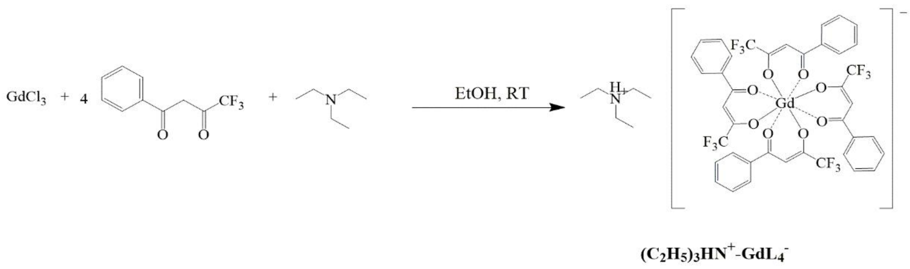

Scheme S2 Synthesis of $(C_2H_5)_3HN^+$-GdL_4^-

ABM (1.8 mmol, 0.3891g) was added into 5 mL of hot ethanol until dissolved, 0.2509 mL (1.8 mmol) triethylamine was dropped into the ABM solution, then 0.4 mmol of $GdCl_3$ in 2 mL of water was added. The solution was allowed to react at room temperature for 2.5 h with stirring. The mixed solution was separated into two layers and the oily substance appears at the bottom. Such oily substance was collected after liquid separation and was cooled in an ice bath. Finally, the solid of $(C_2H_5)_3HN^+$-GdL_4^- was obtained. The crude product was washed with excessive *n*-hexane for 3 times. Then the product was dried in vacuum, the light-yellow product with a yield of 94% was obtained.

Synthesis of TPE$^+$-EuL$_4^-$(L=ABM)

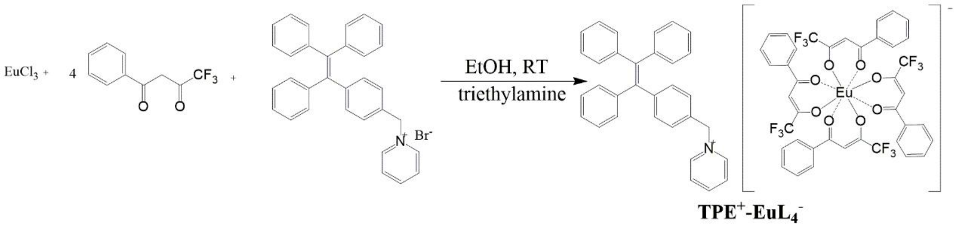

Scheme S3 Synthesis of TPE$^+$-EuL$_4^-$

ABM (1.8 mmol, 0.3891g) and TPE$^+$-Br$^-$ (0.4 mmol, 0.2016g) was added into 6 mL of hot ethanol, 0.2509 mL (1.8 mmol) triethylamine was dropped into the above solution, then 0.4 mmol of $EuCl_3$ in 2 mL of water was added. The solution was allowed to react at room temperature for 1.5 h with stirring. The crude product was collected by filtration and washed with excessive *n*-hexane for 3 times. And then it was dried using the P_2O_5. Finally, TPE$^+$-EuL$_4^-$ with a yield of 90% was obtained.

Synthesis of TPE$^+$-GdL'$_4^-$(L'=CA)

The procedure was very similar as the synthesis of TPE$^+$-EuL$_4^-$(L=ABM). The differences were ABM was replaced by citric acid (CA) and $EuCl_3$ was substituted by $GdCl_3$. Finally, the ready-to-use product of TPE$^+$-GdL'$_4^-$ (L'=CA) was obtained.

Captions

Fig. S1 ^1H NMR spectrum of the 1-(4-(1,2,2-triphenylvinyl)benzyl)pyridin-1-ium bromide (denoted as TPE^+-Br^-) in $CDCl_3$.

Fig. S2 ESI-Mass spectrum of TPE^+-Br^-.

Fig. S3 SEM image of TPE^+-Br^-.

Fig. S4 AIE behavior (a) and plots of the fluorescence intensity at 435 nm of TPE^+-Br^- dissolved in THF/*n*-hexane mixtures with different *n*-hexane fractions (λ_{ex}=350 nm) (Inset : Digital photos under 365 nm UV light)(b).

Fig. S5 TEM image of TPE^+-EuL_4^- in *n*-hexane (L=ABM).

Fig. S6 The XPS survey spectra of TPE^+-EuL_4^- (L=ABM).

Fig. S7 XRD patterns of the TPE^+-EuL_4^-, $(C_2H_5)_3NH^+$-$EuL_4^-$and TPE^+-Br^-(L=ABM).

Fig. S8 FT-IR spectra of ABM, TPE^+-Br^- and TPE^+-EuL_4^-(L=ABM).

Fig. S9 Emission spectra of TPE^+-Br^- and TPE^+-EuL_4^- dissolved in DMF/H_2O (f_w=90%) (λ_{ex}=385 nm)(L=ABM).

Fig. S10 UV-vis spectra of $(C_2H_5)_3HN^+$-GdL_4^- and TPE^+-$GdL'_4{}^-$ under 77K (L=ABM; L'=citric acid).

Fig. S11 Phosphorescence spectra of $(C_2H_5)_3HN^+$-GdL_4^- and TPE^+-$GdL'_4{}^-$ under 77K (L=ABM; L'=citric acid).

Fig. S12 Energy transfer mechanism in TPE^+-EuL_4^- (L=ABM).

Fig. S13 RT fluorescence decay curves of TPE^+-$GdL'_4{}^-$ (L'=citric acid) and TPE^+-EuL_4^- (L=ABM) in DMF/H_2O (f_w=90%) (excited at 350 nm and observed at 467 nm).

Fig. S14 RT fluorescence decay curves of $(C_2H_5)_3HN^+$-EuL_4^- and TPE^+-EuL_4^- (L=ABM) in DMF/H_2O (f_w=90%) (excited at 350 nm and observed at 614 nm).

Fig. S15 Excitation spectra of $(C_2H_5)_3HN^+$-EuL_4^- (λ_{em}=614 nm), TPE^+-Br^- (λ_{em}=435 nm) and TPE^+-EuL_4^- solid(L=ABM) (λ_{em}=614 nm).

Fig. S16 Excitation spectra of TPE^+-EuL_4^- materials dissolved in DMF/water mixtures with different water fractions (λ_{em}=614 nm)(L=ABM).

Fig. S17 UV-vis spectra of TPE^+-EuL_4^-(1.0×10^{-4} mol/L) in DMF/H_2O (f_w=50%) upon addition of ATP^{2-}(L=ABM)(a);The ratio of the intensity about the Uv-vis absorption peaks located at 323 nm and 256 nm when the concentration of ATP^{2-} increased.(b)

Fig. S18 UV-vis spectra of of ATP^{2-} (2.0×10^{-4} mol/L) and PAA-1(M_W=1450000) (0.2 mg/mL) in water.

Fig. S19 Fluorescence of TPE-ATP compound generated by TPE^+ and ATP^{2-} (red line) and TPE^+-EuL_4^- (L=ABM) (black line) dissolved in DMF/H_2O (f_w=90%)(λ_{ex}=385 nm).

Fig. S20 UV-vis spectra of TPE^+-EuL_4^- in DMF/H_2O (f_w=50%) in presence of different anions (ATP^{2-}, $H_2PO_2^-$, HPO_3^{2-}, $H_2PO_4^-$ and $P_2O_7^{4-}$) (200 μM).

Fig. S21 Emission spectra of TPE^+-EuL_4^-(1.0×10^{-4} mol/L) in DMF/H_2O (f_w=90%) upon addition of $H_2PO_2^-$ (L=ABM) (λ_{ex}=385 nm).

Fig. S22 Emission spectra of TPE^+-EuL_4^-(1.0×10^{-4} mol/L) in DMF/H_2O (f_w=90%) upon addition of HPO_3^{2-} (L=ABM) (λ_{ex}=385 nm).

Fig. S23 Emission spectra of TPE^+-EuL_4^-(1.0×10^{-4} mol/L) in DMF/H_2O (f_w=90%) upon addition of $H_2PO_4^-$ (L=ABM) (λ_{ex}=385 nm).

Fig. S24 Emission spectra of TPE^+-EuL_4^-(1.0×10^{-4} mol/L) in DMF/H_2O (f_w=90%) upon addition of $P_2O_7^{4-}$ (L=ABM) (λ_{ex}=385 nm).

Fig. S25 UV-vis spectra of TPE^+-EuL_4^- (1.0×10^{-4} mol/L) in DMF/H_2O (f_w=50%) upon addition of PAA-1 (M_W=1450000) (L=ABM)(a); The ratio of the intensity about the Uv-vis absorption peaks located at 323 nm and 256 nm when the amount of PAA increased (b).

Fig. S26 Emission spectra of TPE^+-EuL_4^- (1.0×10^{-4} mol/L) in DMF/H_2O (f_w=90%) upon addition of PAA-2 (M_W=3000) (L=ABM) (λ_{ex}=320 nm).

Fig. S27 Emission spectra of TPE^+-EuL_4^- (1.0×10^{-4} mol/L) in DMF/H_2O (f_w=90%) upon addition of AA (L=ABM) (λ_{ex}=320 nm).

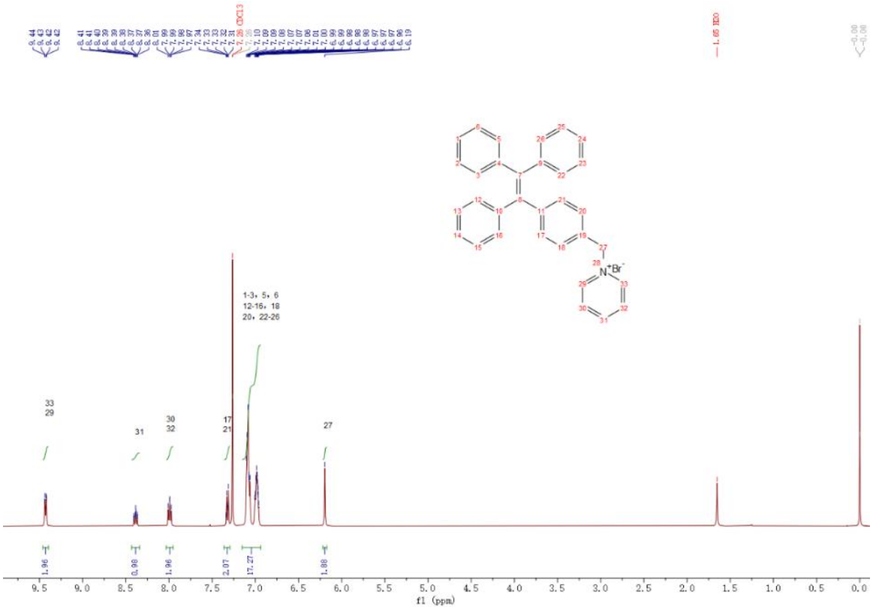

Fig. S1 ^{1}H NMR spectrum of the 1-(4-(1,2,2-triphenylvinyl)benzyl)pyridin-1-ium bromide (denoted as TPE^{+}-Br^{-}) in CDCl$_3$.

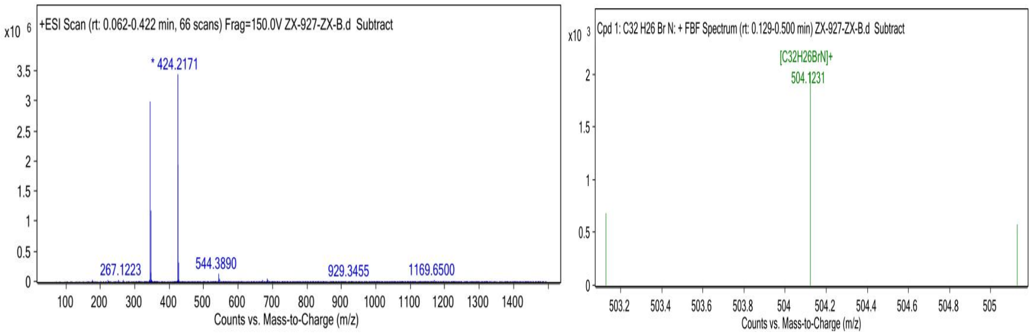

Fig. S2 ESI-Mass spectrum of TPE^{+}-Br^{-}.

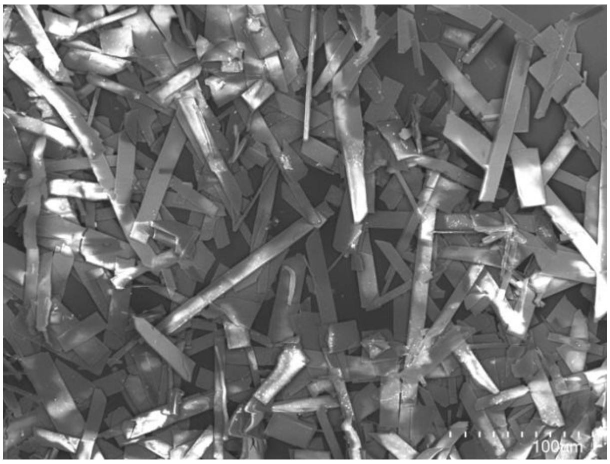

Fig. S3 SEM image of TPE^{+}-Br^{-}.

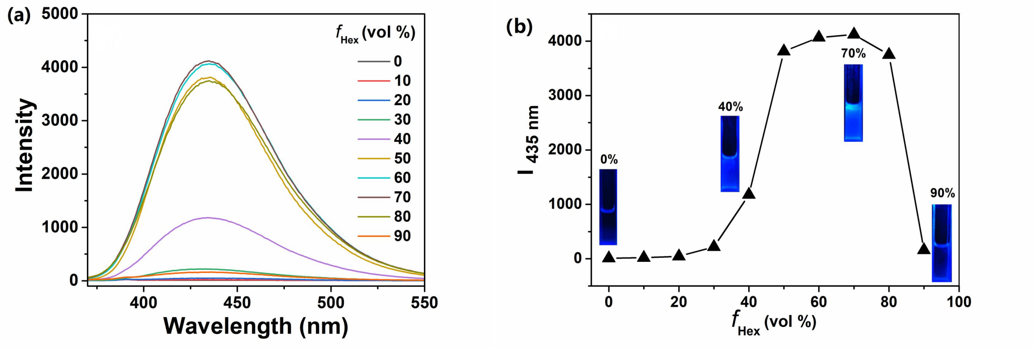

Fig. S4 AIE behavior (a) and plots of the fluorescence intensity at 435 nm of TPE^+-Br^- dissolved in THF/*n*-hexane mixtures with different *n*-hexane fractions (λ_{ex}=350 nm) (Inset : Digital photos under 365 nm UV light)(b).

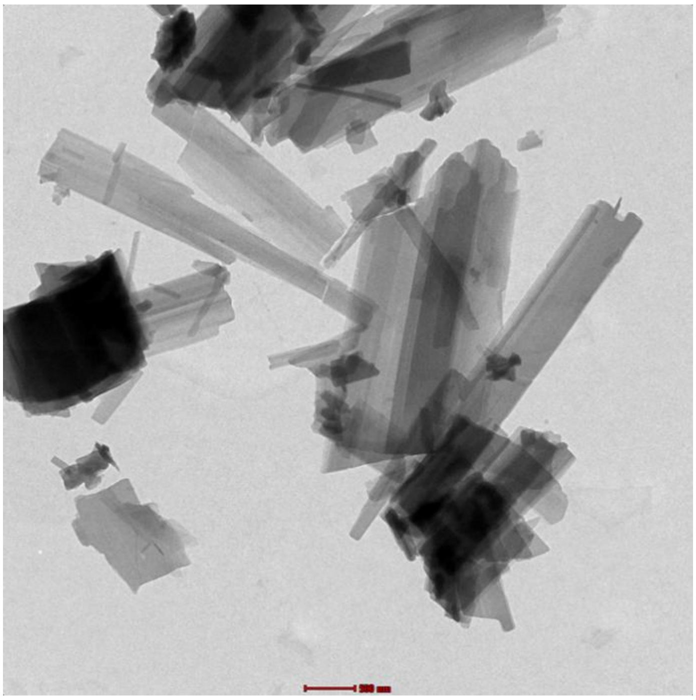

Fig. S5 TEM image of TPE^{+}-EuL_4^{-} in *n*-hexane (L=ABM).

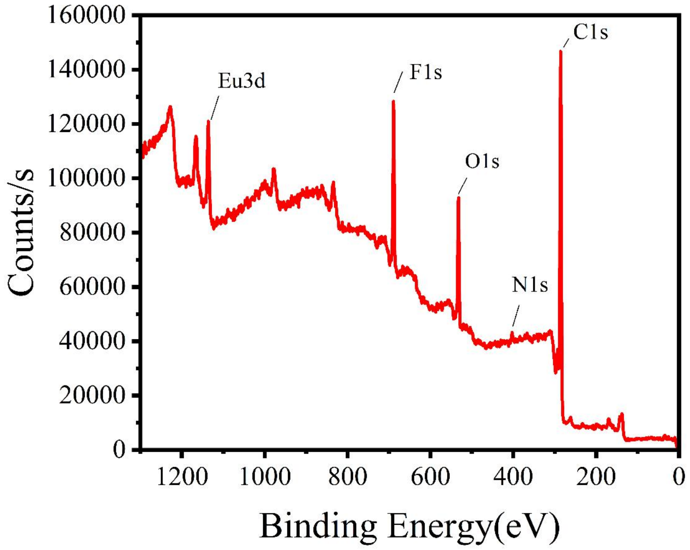

Fig. S6 The XPS survey spectra of TPE$^+$-EuL$_4$$^-$ (L=ABM).

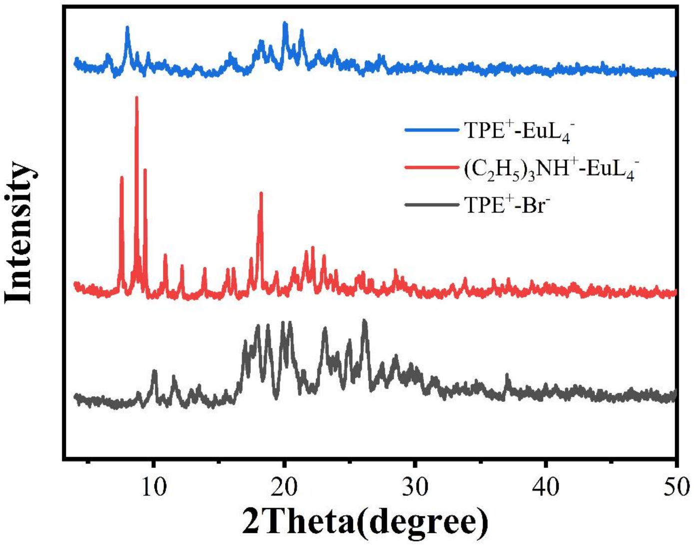

Fig. S7 XRD patterns of the TPE$^+$-EuL$_4^-$, (C$_2$H$_5$)$_3$NH$^+$-EuL$_4^-$and TPE$^+$-Br$^-$(L=ABM).

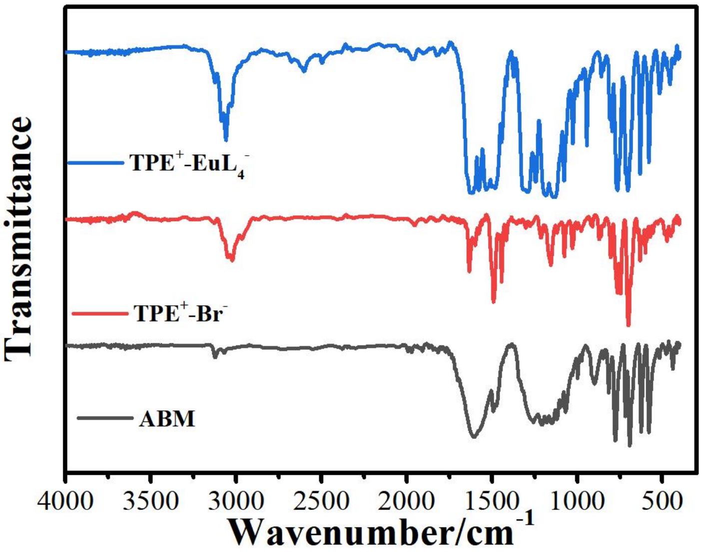

Fig. S8 FT-IR spectra of ABM, TPE^+-Br^- and TPE^+-EuL_4^-(L=ABM).

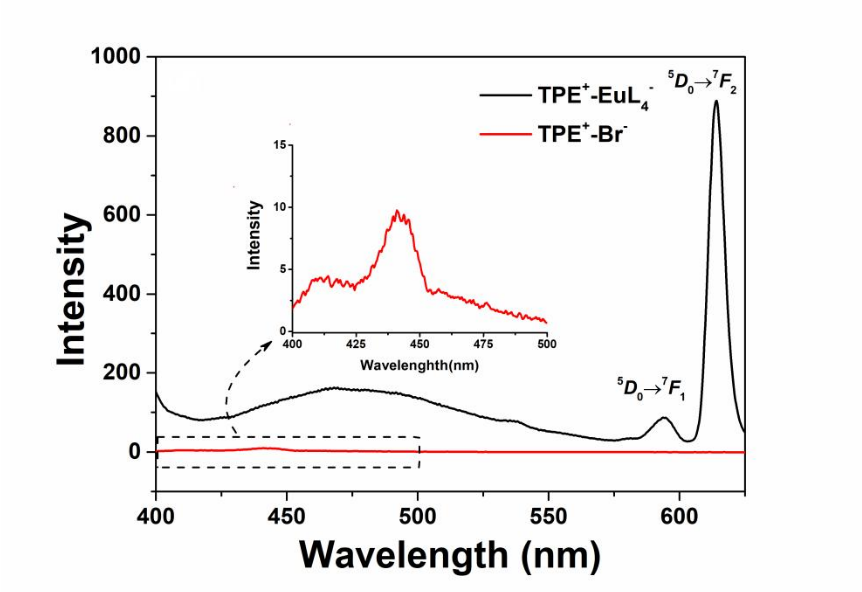

Fig. S9 Emission spectra of TPE$^+$-Br$^-$ and TPE$^+$-EuL$_4$$^-$ dissolved in DMF/H$_2$O (f_w=90%) (λ_{ex}=385 nm) (L=ABM).

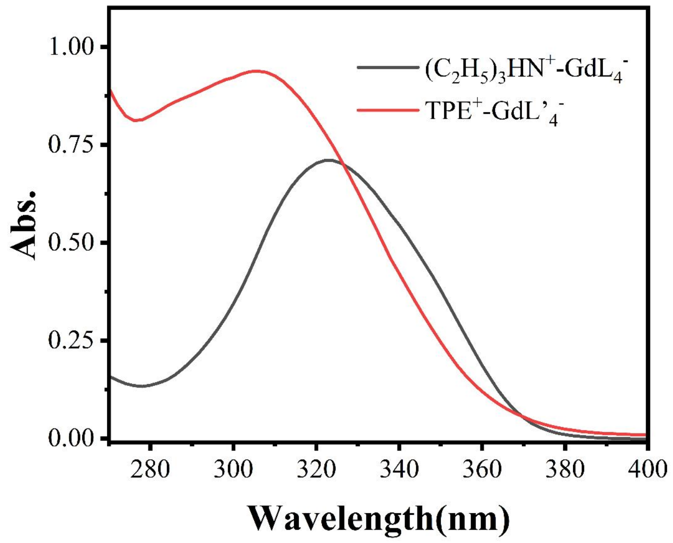

Fig. S10 UV-vis spectra of $(C_2H_5)_3HN^+$-GdL_4^- and TPE^+-GdL'^-_4 under 77K (L=ABM; L'=citric acid).

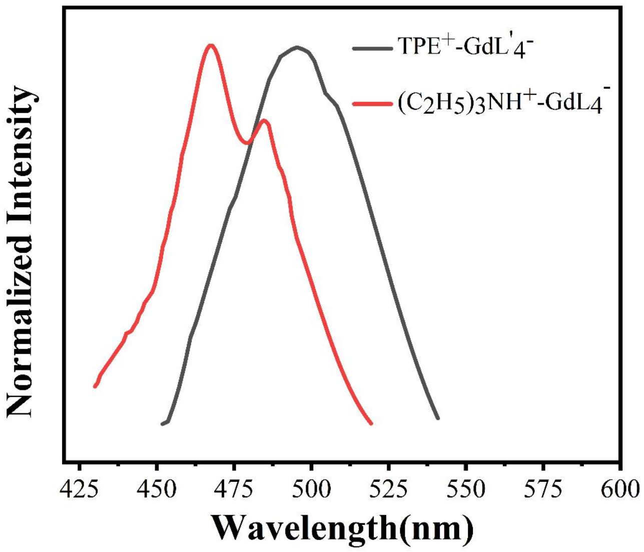

Fig. S11 Phosphorescence spectra of $(C_2H_5)_3HN^+$-GdL$_4^-$ and TPE$^+$-GdL'$_4^-$ under 77K (L=ABM; L'=citric acid).

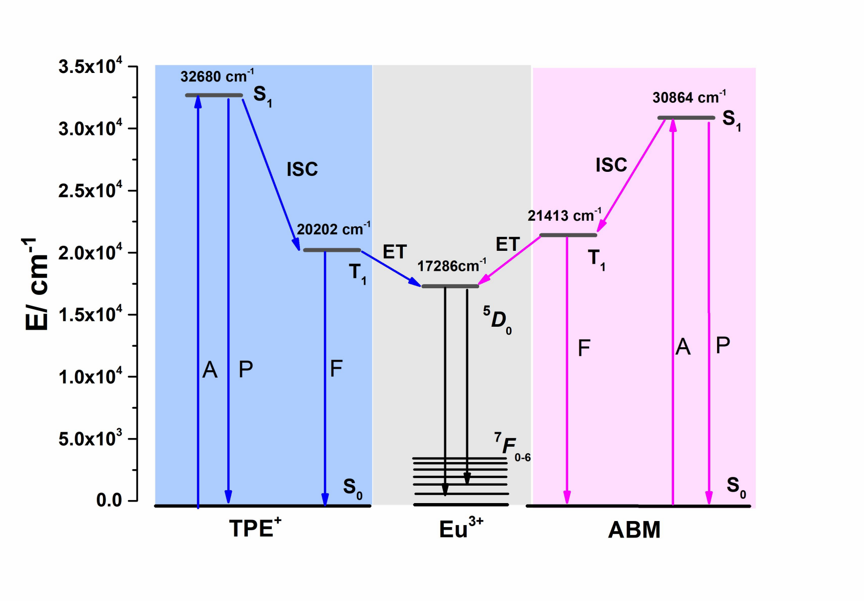

Fig. S12 Energy transfer mechanism in TPE^+-EuL_4^-(L=ABM).

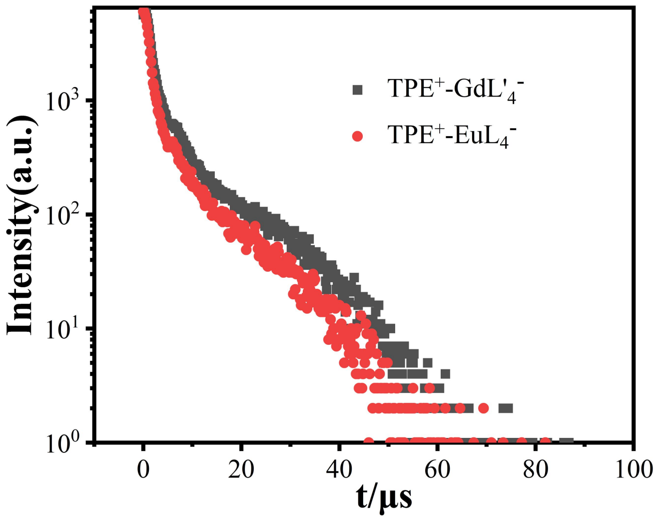

	TPE^+-$GdL'_4{}^-$	TPE^+-$EuL_4{}^-$
A_1	6742.791	7300.465
A2	768.299	563.869
τ_f (μs)	1.268	1.0924
τ_s (μs)	10.8710	9.6564
τ_{av} (μs)	6.01	4.56

Fitting curve formula $R(t)=A_0+A_1e^{(-t/\tau f)}+A_2e^{(-t/\tau s)}$

$\tau_{av}=\frac{\tau_f{}^2A_1+\tau_s{}^2A_2}{\tau_f A_1+\tau_s A_2}$ where, the τ_f is the fast decay time and the τ_s slow decay time.

Fig. S13 RT fluorescence decay curves of TPE^+-$GdL'_4{}^-$ (L'=citric acid) and TPE^+-$EuL_4{}^-$ (L=ABM) in DMF/H_2O (f_w=90%) (excited at 350 nm and observed at 467 nm).

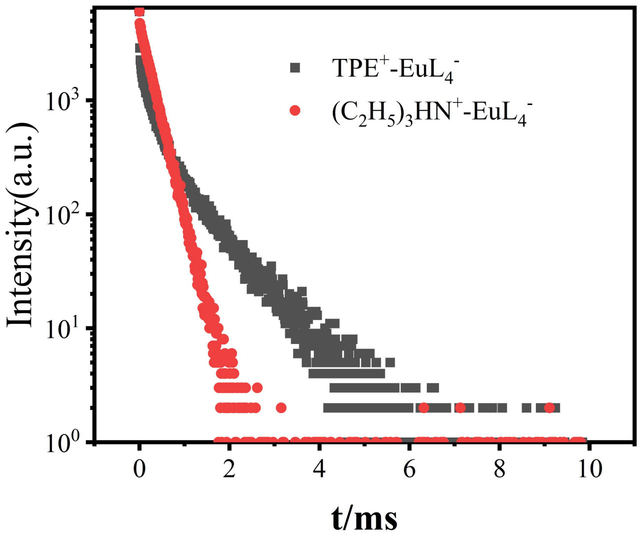

	$(C_2H_5)_3HN^+$-EuL$_4^-$	TPE$^+$-EuL$_4^-$
A_1	6586.582	2042.330
A_2	4875.186	745.668
τ_f (μs)	6.2246	137.0661
τ_s (μs)	257.7839	699.9999
τ_{av} (μs)	249.8	503.5

Fitting curve formula $R(t)=A_0+A_1e^{(-t/\tau f)}+A_2e^{(-t/\tau s)}$

$\tau_{av}=\frac{\tau_f{}^2A_1+\tau_s{}^2A_2}{\tau_fA_1+\tau_sA_2}$ τ_f is fast decay time and τ_s is slow decay time

Fig. S14 RT fluorescence decay curves of $(C_2H_5)_3HN^+$-EuL$_4^-$ and TPE$^+$-EuL$_4^-$ (L=ABM) in DMF/H$_2$O (*f*$_w$=90%) (excited at 350 nm and observed at 614 nm).

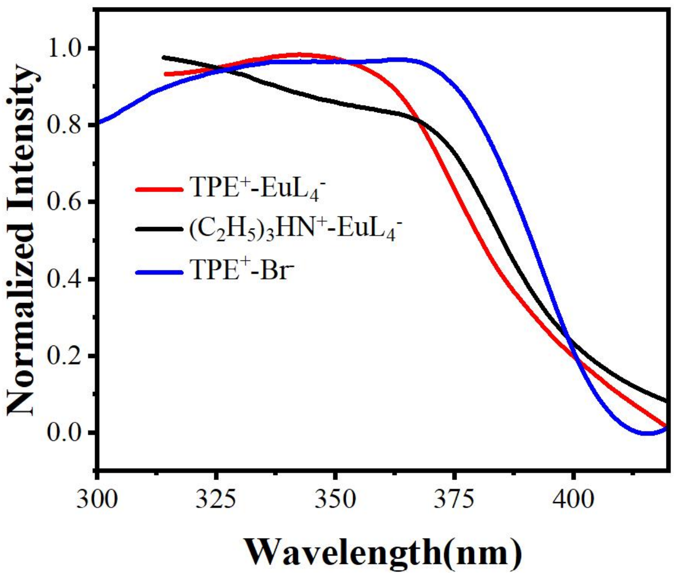

Fig. S15 Excitation spectra of $(C_2H_5)_3HN^+$-EuL_4^- (λ_{em}=614 nm), TPE^+-Br^- (λ_{em}=435 nm) and TPE^+-EuL_4^- solid (L=ABM) (λ_{em}=614 nm).

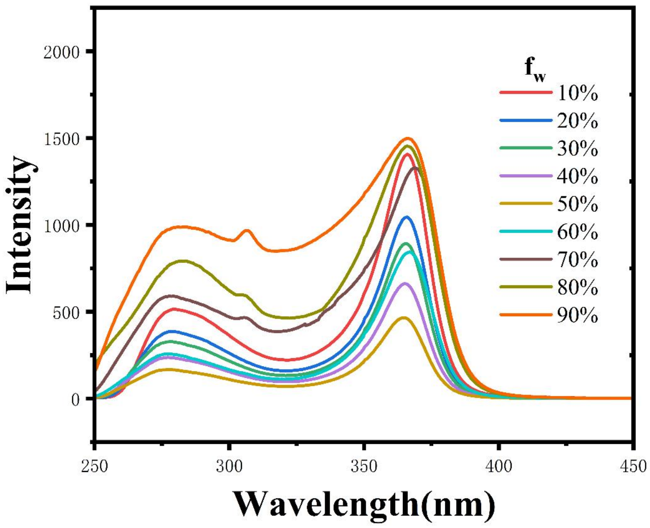

Fig. S16 Excitation spectra of TPE$^+$-EuL$_4^-$ materials dissolved in DMF/water mixtures with different water fractions (λ_{em}=614 nm)(L=ABM).

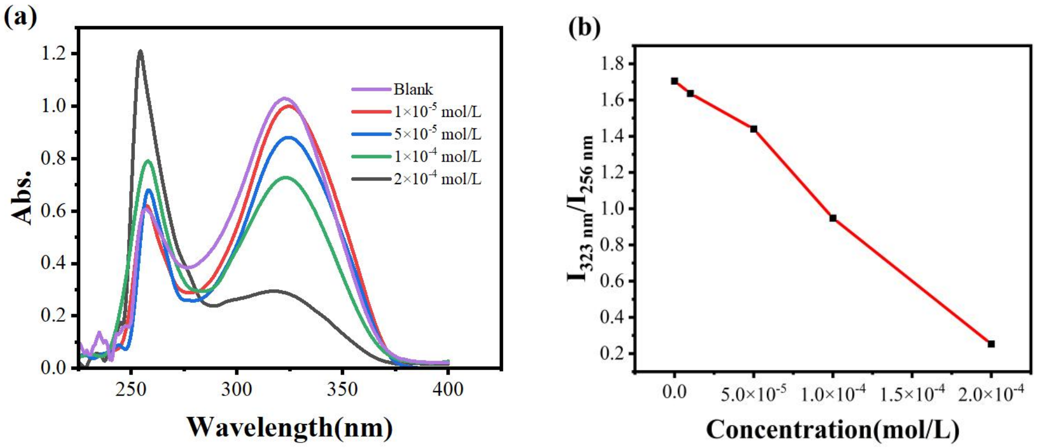

Fig. S17 UV-vis spectra of TPE$^+$-EuL$_4^-$(1.0×10^{-4} mol/L) in DMF/H$_2$O (f_w=50%) upon addition of ATP^{2-}(L=ABM)(a); The ratio of the intensity about the Uv-vis absorption peaks located at 323 nm and 256 nm when the concentration of ATP^{2-} increased (b).

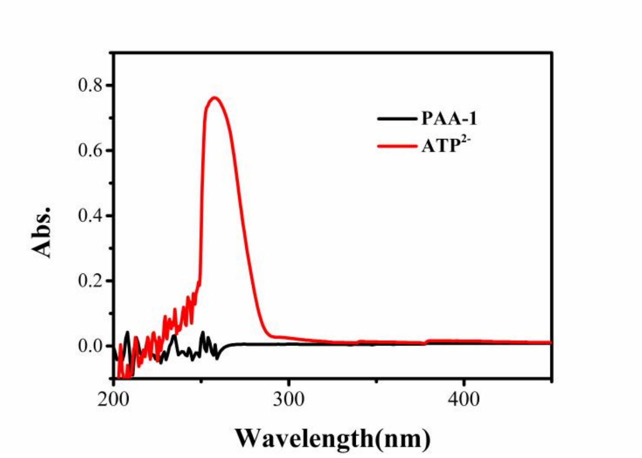

Fig. S18 UV-vis spectra of of ATP^{2-} (2.0×10^{-4} mol/L) and PAA-1(M_W=1450000) (0.2 mg/mL) in water.

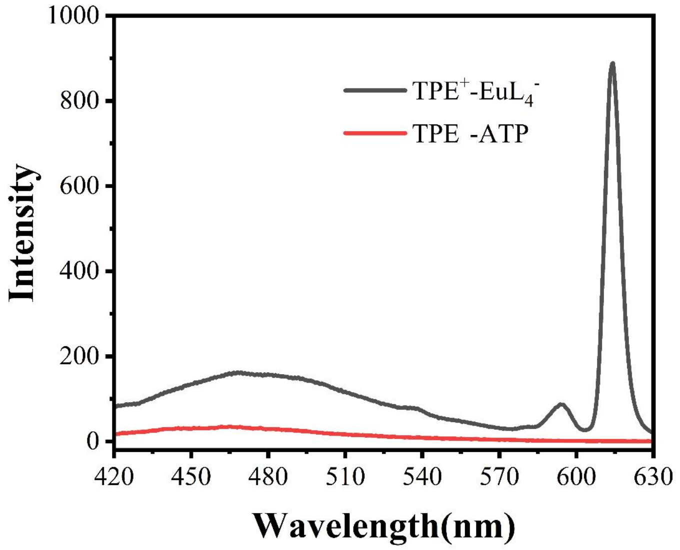

Fig. S19 Fluorescence of TPE-ATP compound generated by TPE$^+$ and ATP^{2-} (red line) and TPE$^+$-EuL$_4^-$ (L=ABM) (black line) dissolved in DMF/H_2O (f_w=90%)(λ_{ex}=385 nm).

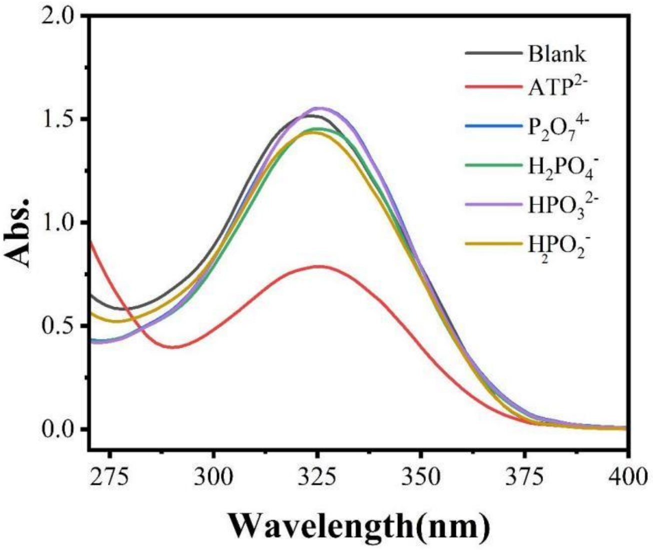

Fig. S20 UV-vis spectra of TPE$^+$-EuL$_4^-$ in DMF/H_2O (f_w=50%) in presence of different anions (ATP^{2-}, $H_2PO_2^-$, HPO_3^{2-} , $H_2PO_4^-$ and $P_2O_7^{4-}$) (200 μM).

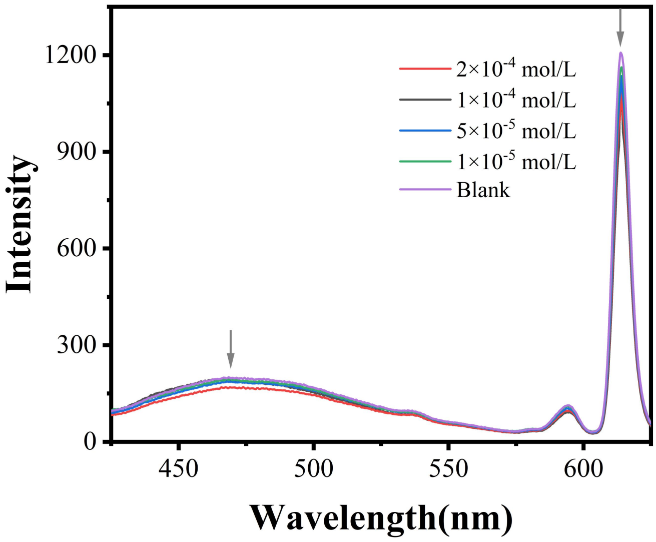

Fig. S21 Emission spectra of TPE^+-EuL_4^-(1.0×10^{-4} mol/L) in DMF/H_2O (f_w=90%) upon addition of $H_2PO_2^-$ (L=ABM) (λ_{ex}=385 nm).

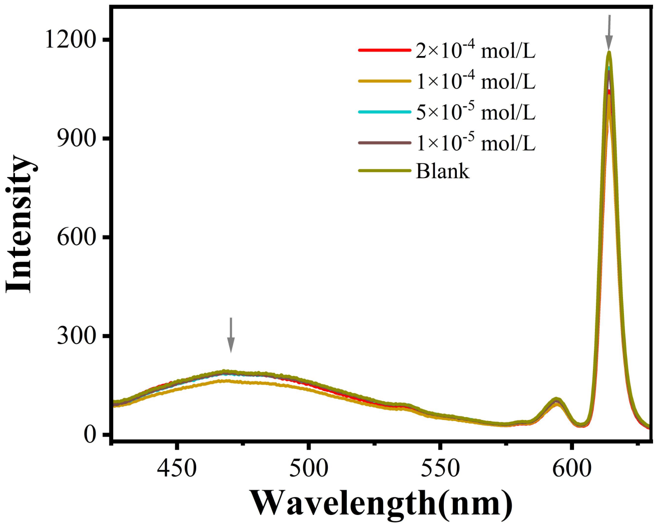

Fig. S22 Emission spectra of TPE$^+$-EuL$_4^-$(1.0×10^{-4} mol/L) in DMF/H$_2$O (f_w=90%) upon addition of HPO$_3^{2-}$ (L=ABM) (λ_{ex}=385 nm).

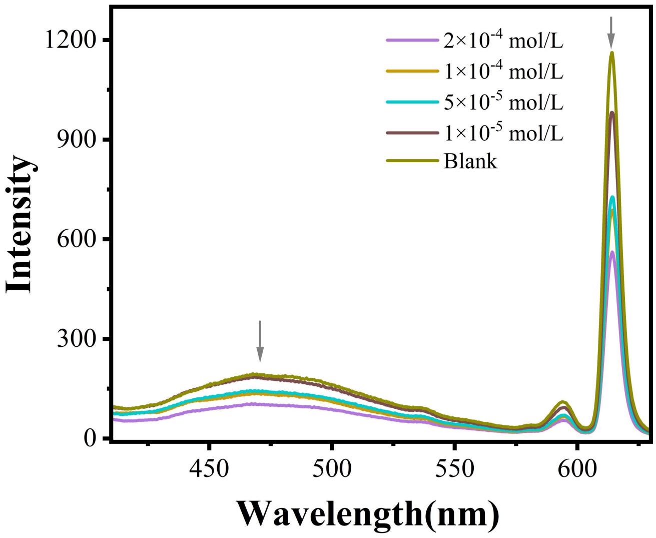

Fig. S23 Emission spectra of TPE$^+$-EuL$_4^-$(1.0×10^{-4} mol/L) in DMF/H$_2$O (f_w=90%) upon addition of H$_2$PO$_4^-$ (L=ABM) (λ_{ex}=385 nm).

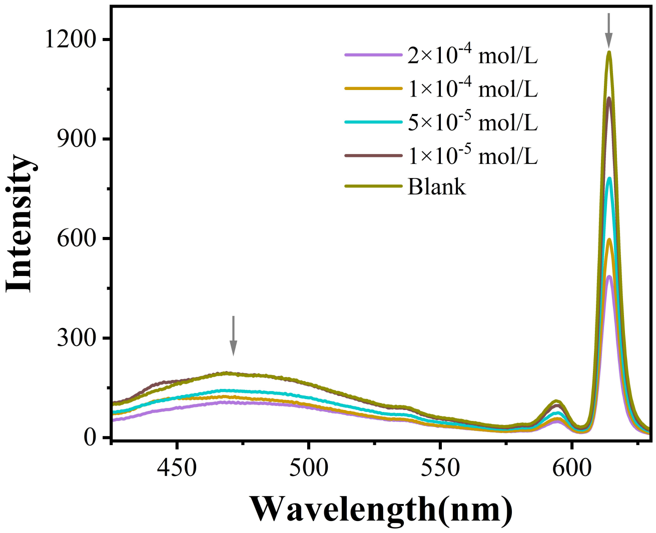

Fig. S24 Emission spectra of TPE^{+}-EuL$_4^{-}$(1.0×10^{-4} mol/L) in DMF/H$_2$O (f_w=90%) upon addition of P$_2$O$_7^{4-}$ (L=ABM) (λ_{ex}=385 nm).

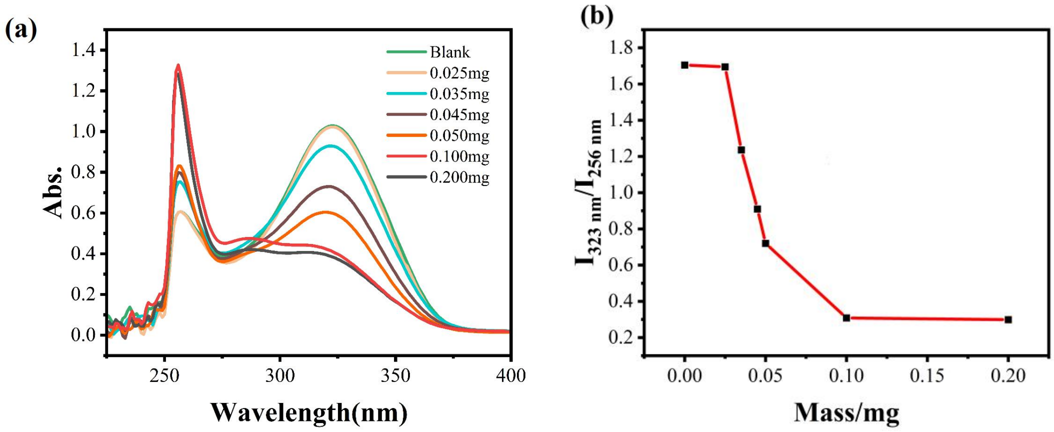

Fig. S25 UV-vis spectra of TPE$^+$-EuL$_4^-$ (1.0×10^{-4} mol/L) in DMF/H$_2$O (f_w=50%) upon addition of PAA-1 (MW=1450000) (L=ABM)(a); The ratio of the intensity about the Uv-vis absorption peaks located at 323 nm and 256 nm when the amount of PAA increased (b).

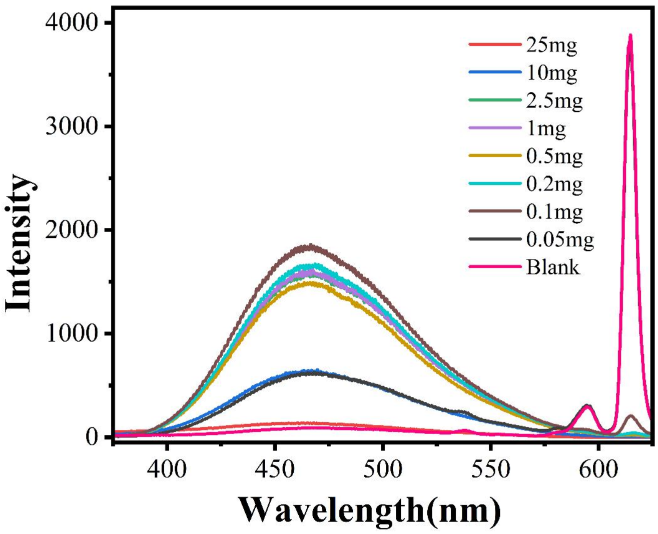

Fig. S26 Emission spectra of TPE$^+$-EuL$_4^-$ (1.0×10^{-4} mol/L) in DMF/H$_2$O (f_w=90%) upon addition of PAA-2 (M$_W$=3000) (L=ABM) (λ_{ex}=320 nm).

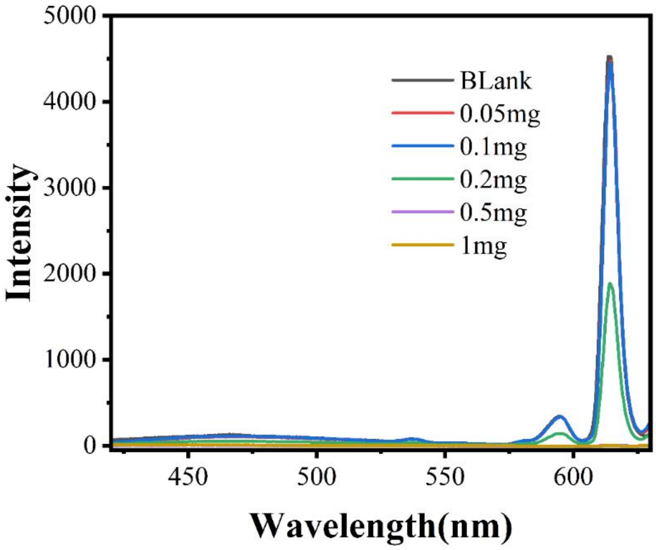

Fig. S27 Emission spectra of TPE$^+$-EuL$_4^-$ (1.0×10^{-4} mol/L) in DMF/H$_2$O (f_w=90%) upon addition of AA (L=ABM) (λ_{ex}=320 nm).

Table. S1 Summary of FT-IR spectra in ABM, TPE$^+$-Br$^-$ and TPE$^+$-EuL$_4^-$(L=ABM).

Compounds	ν(Ar-H)	ν(C=O)	ν(C-F)	ν(C=C)	ν(C=N)	ν(CF$_3$)
ABM	**3126**	**1608**	**1259**	**1493**	/	**815**
TPE$^+$-Br$^-$	**3023**	/	/	**1490**	**1623**	/
TPE$^+$-EuL$_4^-$	**3059**	**1583**	**1297**	**1483**	**1621**	**796**

Table. S2 Elemental analysis in TPE$^+$-Br$^-$, $(C_2H_5)_3HN^+$-EuL$_4^-$ and TPE$^+$-EuL$_4^-$(L=ABM).

		C	H	N	O	Eu
TPE$^+$-Br$^-$	**calculated**	**76.19**	**5.20**	**2.78**	/	/
	found	**76.21**	**5.27**	**2.92**	/	/
$(C_2H_5)_3HN^+$-EuL$_4^-$	**calculated**	**49.56**	**3.62**	**1.261**	**11.48**	**13.63**
	found	**49.53**	**3.637**	**1.29**	**12.01**	**12.93**
TPE$^+$-EuL$_4^-$	**calculated**	**60.07**	**3.51**	**0.97**	**8.91**	**10.57**
	found	**59.67**	**3.83**	**1.04**	**9.28**	**10.74**